

# Journal of Materials Chemistry A

Accepted Manuscript



This is an *Accepted Manuscript*, which has been through the Royal Society of Chemistry peer review process and has been accepted for publication.

*Accepted Manuscripts* are published online shortly after acceptance, before technical editing, formatting and proof reading. Using this free service, authors can make their results available to the community, in citable form, before we publish the edited article. We will replace this *Accepted Manuscript* with the edited and formatted *Advance Article* as soon as it is available.

You can find more information about *Accepted Manuscripts* in the [Information for Authors](#).

Please note that technical editing may introduce minor changes to the text and/or graphics, which may alter content. The journal's standard [Terms & Conditions](#) and the [Ethical guidelines](#) still apply. In no event shall the Royal Society of Chemistry be held responsible for any errors or omissions in this *Accepted Manuscript* or any consequences arising from the use of any information it contains.



## Defining a performance map of porous carbon sorbents for high-pressure carbon dioxide uptake and carbon dioxide-methane selectivity

Received 00th January 20xx,  
Accepted 00th January 20xx

DOI: 10.1039/x0xx00000x

www.rsc.org/

Saunab Ghosh,<sup>a</sup> Marta Sevilla,<sup>b</sup> Antonio B. Fuentes,<sup>\*b</sup> Enrico Andreoli,<sup>\*c</sup> Jason Ho,<sup>d</sup> and Andrew R. Barron<sup>\*a,c,e</sup>

The relative influence of heteroatom doping, surface area, and total pore volume of highly microporous carbon materials on CO<sub>2</sub> uptake capacity, and the CO<sub>2</sub>/CH<sub>4</sub> selectivity, at high pressure (≤30 bar) is presented. The separation of CO<sub>2</sub> from natural gas (natural gas sweetening) is an important application that requires high CO<sub>2</sub> uptake in combination with high CO<sub>2</sub>/CH<sub>4</sub> selectivity. Porous carbon (PC), N-doped PC (NPC), and S-doped PC (SPC) materials are prepared using KOH oxidative activation at different temperatures. The surface chemical composition was determined by XPS, while the surface areas, total pore volume, and pore size distributions were obtained by analyzing N<sub>2</sub> adsorption-desorption isotherms with support from SEM and TEM. The CO<sub>2</sub> and CH<sub>4</sub> uptake was determined by volumetric uptake measurements (sorption and desorption). Contrary to previous proposals that N- or S-doping results in high uptake and good selectivity, we show it is the Σ(O,N,S) wt% that is the defining factor for CO<sub>2</sub> uptake, of which O appears to be the main factor. Based upon the data analyzed, a performance map has been defined as a guide to designing/choosing materials for both future studies and large scale fluid bed applications using pelletized materials. For CO<sub>2</sub> uptake at 30 bar any material with a surface area >2800 m<sup>2</sup>g<sup>-1</sup> and a total pore volume >1.35 cm<sup>3</sup>g<sup>-1</sup> is unlikely to be bettered. Such a material is best prepared by thermal activation between 700-800 °C and will have a carbon content of 80-95 wt% (as determined by XPS). While it has been assumed that the parameters that make a good CO<sub>2</sub> adsorbent are the same as those that make a material with high CO<sub>2</sub>/CH<sub>4</sub> selectivity, our results indicate instead that for the best selectivity at 30 bar a surface area >2000 m<sup>2</sup>g<sup>-1</sup> and a total pore volume >1.0 cm<sup>3</sup>g<sup>-1</sup> and a carbon content of <90 wt% are necessary.

### 1. Introduction

An historic agreement was achieved between 55 countries, at the COP21 meeting in Paris in 2015, to limit the global temperature rise associated with climate change to 1.5 °C. The agreement calls for zero net anthropogenic greenhouse gas emissions to be reached during the second half of the 21<sup>st</sup>

century.<sup>1-4</sup> Basically, three approaches can be envisaged for lowering global CO<sub>2</sub>: a) decreasing emissions, b) carbon capture and storage (CCS), including both biological and geological sequestration, and c) chemical conversion to alternative useful compounds. While the first of these approaches is generally the one politically mandated, it is important to note that lowering local emissions does not necessarily equate to lowering global emissions.<sup>5</sup> For example, lithium mining and processing for batteries to replace internal combustion engines requires significant energy and chemical waste at locations remote from the end use. Thus, while long term lowering of global emissions is clearly desirable, and chemical conversion may reduce the use of other raw materials, CCS offers the best near-term possibility until global infrastructure has evolved.<sup>6</sup>

Of the multiple approaches for CCS each has advantages and disadvantages in terms of capacity, cost, the time scale of the sequestration, the stability of sequestered CO<sub>2</sub>, and additional environmental impacts, which depend on the location, time, and amount of sequestration.<sup>7</sup> There has been much made of biological sequestration as being a natural approach; however, despite this obvious advantage it is now

<sup>a</sup> Department of Chemistry, Rice University, Houston, Texas 77007, USA.

<sup>b</sup> Instituto Nacional del Carbón (CSIC), P.O. Box 73, Oviedo 33080, Spain.

<sup>c</sup> Energy Safety Research Institute, Swansea University, Bay Campus, Swansea, SA1 8XX, Wales, UK.

<sup>d</sup> Apache Corporation, 2000 Post Oak Blvd., Houston, TX 77056, USA

<sup>e</sup> Department of Materials Science and Nanoengineering, Rice University, Houston, Texas 77007, USA.

\*Corresponding authors E-mail: [abefu@incar.csic.es](mailto:abefu@incar.csic.es) (A. B. Fuentes), [e.andreoli@swansea.ac.uk](mailto:e.andreoli@swansea.ac.uk) (E. Andreoli), [arb@rice.edu](mailto:arb@rice.edu); [a.r.barron@swansea.ac.uk](mailto:a.r.barron@swansea.ac.uk) (A. R. Barron).

Electronic Supplementary Information (ESI) available: Plots of high pressure CO<sub>2</sub> uptake measurements, surface area and total pore volume as a function of activation temperature, distribution of pore volumes as a function of pore width, CO<sub>2</sub> and CH<sub>4</sub> adsorption uptake measurements for PC and NPC samples; FTIR for NPC and SPC samples. See DOI: 10.1039/x0xx00000x

known that there are significant disadvantages such as CH<sub>4</sub> emissions.<sup>8</sup>

While sequestration of global CO<sub>2</sub> emissions may in-part be achieved through natural sinking rates of CO<sub>2</sub>,<sup>9</sup> those produced at anthropogenic sources require a more directed approach. Key to such sequestration is the separation of CO<sub>2</sub> from gas mixtures, such as the abatement of CO<sub>2</sub> in flue gas (from N<sub>2</sub> and H<sub>2</sub>O).<sup>10,11</sup> However, another less discussed area is the separation of CO<sub>2</sub> from natural gas (natural gas sweetening).<sup>12,13</sup> Although CH<sub>4</sub> (the main component of natural gas) is itself a greenhouse gas, as recovered from wells, natural gas produced globally has significant CO<sub>2</sub> content (as high as 50%).<sup>14</sup> This CO<sub>2</sub> must be removed from the gas prior to its use since it is a major source of corrosion. Key attributes for natural gas treatment include: a) high CO<sub>2</sub> uptake; b) high selectivity; c) minimal or no deactivation upon cycling; d) ability to work at high pressures and at or above ambient temperatures.

There are generally two classes of material employed for CO<sub>2</sub> separation: reactants and adsorbents. The former includes amine and other reactive species such as ionic liquids and alkali-metal-based oxides. At present, monoethanolamine (MEA) is the industry standard; however, regeneration, degradation and corrosion, together with health and environmental issues, still affect its large scale implementation.<sup>15-18</sup> Impregnation onto supports has been investigated,<sup>19-21</sup> but it is only recently that the regeneration temperature has been lowered by their combination with carbon nanomaterials.<sup>22-24</sup> Ionic liquids, suitable for high pressure capture are expensive and toxic,<sup>25,26</sup> while cheap alkali metal oxides suffer from severe deactivation upon cycling.<sup>27</sup> Although these materials show excellent selectivity between CO<sub>2</sub> and CH<sub>4</sub>, their myriad drawbacks have meant that much effort has been invested into the study of solid porous sorbents,<sup>28</sup> such as porous carbons (PC),<sup>29</sup> metal-organic frameworks (MOFs),<sup>30,31</sup> microporous zeolites,<sup>21,32</sup> and porous silica-based sorbents with high surface area.<sup>33</sup>

MOFs outperform zeolites in terms of maximum capacity at high pressure,<sup>20,34</sup> but are rather expensive as they require complex multistep synthesis procedures. In addition, their gas adsorption capacity degrades after several cycles of usage. Carbonaceous materials, such as activated carbon and charcoal, are cheaper and less sensitive to moisture than zeolites and MOFs, but their adsorption capacity generally increases with loss of selectivity at high pressure.<sup>20,28</sup>

Chemically activated porous carbon (PC) adsorbents have large surface areas and pore volumes associated with micro- and meso-porous structure, and as a result show significantly improved CO<sub>2</sub> capturing capacity as compared to traditional carbonaceous materials.<sup>35-41</sup> While these materials have been extensively studied, there has been a recent report that dramatic increases in both CO<sub>2</sub>:CH<sub>4</sub> selectivity and uptake are observed with either nitrogen- or sulphur-containing chemically activated PCs (NPC and SPC, respectively).<sup>41</sup> These studies were undertaken at 30 bar (1 bar = 100,000 Pa = 750.06 mmHg) using compounds previously reported to show improved results over activated carbon at 1 bar.<sup>35,36,42</sup>

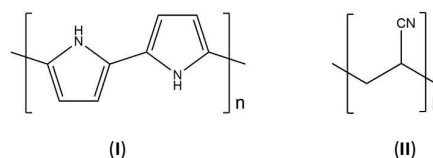
However, the improved high pressure results were proposed to be due to the S or N centres acting as a Lewis base to facilitate the ambient polymerization of the CO<sub>2</sub>. However, computational studies<sup>43</sup> and comparison with prior model compounds,<sup>44,45</sup> suggest that if such poly-CO<sub>2</sub> species are formed then both Lewis acid and Lewis base moieties are needed. Irrespective of the explanation, it is of interest to determine what features of a porous carbon material result in high uptake and good selectivity. We have previously investigated the role of N-doping in CO<sub>2</sub> capture by PCs up to 1 bar pressure and shown no correlation.<sup>37</sup> This has been confirmed by a recent extensive study by Adeniran and Mokaya.<sup>46</sup> Nevertheless, in our prior studies with nano adsorbents at high pressures<sup>47</sup> we have observed that measurements at 1 bar pressure often make it difficult to compare series of similar materials. When measurements at 30 bar are performed, a clearer differentiation between subtle changes in processing conditions can be made. High pressures are also more appropriate when considering applications for natural gas treatment.<sup>48-51</sup>

Herein, we report the study of a range of chemically activated porous carbon materials at high pressure and ambient temperatures in order to determine whether the presence of either S- or N-doping is important in the synthesis of a PC with high uptake and good CO<sub>2</sub>:CH<sub>4</sub> selectivity. It is natural to conclude that high uptake is correlated with high pore volume (and surface area);<sup>37</sup> however, we are interested in seeing what controls this structural parameter: the composition of the PC, the temperature of processing, or the activation chemistry.

## 2. Experimental

### 2.1. Materials and methods

FeCl<sub>3</sub>, pyrrole (purchased from Sigma Aldrich, 98% purity), CH<sub>3</sub>CN, powdered KOH, distilled water, acetone, HCl, coconut shell, activated charcoal (Mallinckrodt chemical works), BPL virgin granular activated carbon (Calgon Carbon Corp.), Ar (99.9% pure), CO<sub>2</sub> (99.99% pure, Matheson TRIGAS) and CH<sub>4</sub> (99.9% pure). Selected PC sorbents studied including, those prepared from eucalyptus sawdust, S-containing PC (SPC) prepared from synthesized polythiophene (PTh), and N-containing PC (NPC) prepared from either polypyrrole (I, PPy), polyacrylonitrile (II, PAN) or by melamine doping of sawdust hydrochar, synthesized according to protocols described previously.<sup>29,35,36,41,52</sup>



Surface chemical composition of the polymer precursors and PC materials were determined by X-ray photoelectron spectroscopy (XPS). The XPS measurements were carried out in a PHI Quantera scanning XPS microprobe. The wt% of

chemical elements was determined by XPS survey scans with pass energy of 140 eV. For detailed elemental analysis high-resolution multi-cycle elemental scans with pass energy 26 eV was performed. Each spectrum was then deconvoluted by appropriate basis functions. Before spectral fitting, each spectrum was corrected for reference binding energy for C1s to 284.8 eV. Scanning electron microscopic images were obtained by a FEI Quanta 400 ESEM FEG high-resolution field emission scanning electron microscope. The high-resolution TEM images of activated sorbents were obtained by a JEOL 2100 field emission gun transmission electron microscope. The textural properties: surface areas ( $S_{\text{BET}}$ ), total pore volume ( $V_{\text{p}}$ ), and pore size distributions (PSDs) of the carbonaceous materials were obtained by analysing  $\text{N}_2$  adsorption isotherms, measured in a Quantachrome Autosorb-3b BET Surface Analyser at 77 K. The surface area ( $S_{\text{BET}}$ ) was calculated by the multipoint BET (Brunauer–Emmett–Teller) method. Before measurements samples were dried at 130 °C for 12 h under high vacuum in a system equipped with a liquid  $\text{N}_2$  cold trap. Pore size distributions were determined by analysing the data via Non-Local Density Functional Theory (NLDFT).<sup>53</sup>

## 2.2. Synthesis of activated PC from coconut shell

Pieces of dry coconut shell were placed inside a quartz tube/tube furnace setup and carbonized for 1 h at 450 °C, under a flow of Ar (flow rate 500 sccm). The carbonized product (500 mg) was thoroughly mixed with KOH powder (1.0 g). The mixture was then placed inside a quartz tube/tube furnace setup, dried for 20 min and then heated for 1 h at a fixed temperature of 600 °C under continuous flow of Ar (flow rate 600 sccm), washed with distilled water (ca. 4 L) and then with acetone (ca. 1 L) and dried at 80 °C for 12 h.

## 2.3. Synthesis of NPC from polypyrrole

The polymerized carbon precursor polypyrrole was synthesized using  $\text{FeCl}_3$  as catalyst following a modification of our previous methods.<sup>35</sup> In a typical synthesis, a solution of  $\text{FeCl}_3$  (50 g) in  $\text{CH}_3\text{CN}$  (200 mL) was prepared. Then, a solution of pyrrole (5.0 g) in  $\text{CH}_3\text{CN}$  (50 mL) was slowly added to the previous solution. The mixture was stirred for 24 h. The polymerized product was separated by filtration, washed thoroughly with distilled water (ca. 4 L) and then with acetone (ca. 1 L) and dried at 80 °C for 12 h. The yield of the final product was ~98%. The polypyrrole was chemically activated by heating with an excess (2 or 4 fold by weight) of KOH in inert atmosphere. In a typical activation process, polypyrrole (500 mg) was thoroughly mixed with KOH (1.0 g) that had been crushed to a fine powder in a mortar. The mixture was then placed inside a quartz tube within a tube furnace, dried for 20 min and then heated for 1 h at a fixed temperature in the 500–800 °C range, under a flow of Ar (flow rate 600 sccm). The activated samples were then thoroughly washed with diluted HCl (1.4 M, 100 mL) and several times with distilled water until the filtrate attained neutral pH 7. Finally, the activated PC was dried on a hot plate at 70 °C for 12 h.

## 2.4. Volumetric $\text{CO}_2$ and $\text{CH}_4$ uptake measurements

The volumetric uptake measurements (sorption and desorption) of  $\text{CO}_2$  and  $\text{CH}_4$  were performed in an automated Sievert instrument (Setaram PCTPRO).<sup>47</sup> Various PC samples were first crushed into powders and packed in a stainless steel autoclave sample cell. Initial sample pre-treatment was carried out at 130 °C for 1.5 h under high vacuum. The free volume inside the sample cell was determined by a series of calibration procedures done under helium. Gas uptake experiments were carried out with high purity research grade  $\text{CO}_2$  (99.99%) and  $\text{CH}_4$  (99.9%) at 24 °C.

## 3. Results and discussion

We have prepared a range of porous carbon sorbent materials in order to compare the performance as a function of a range of variables, including the precursor, the temperature of pyrolysis and the ratio of KOH:precursor used in the activation step. For simplicity, each sample is given an identifier based upon these variables, i.e., precursor-temperature-KOH:precursor ratio. Thus, a sample prepared from polypyrrole (PPy) at 700 °C with a KOH:polypyrrole ratio of 2:1 is labelled as PPy-700-2.

The simplest materials investigated were prepared from either sawdust (SD) or coconut (CN) husks and should contain no N or S and thus can be compared directly with commercial activated charcoal. In order to ascertain the effects of N-doping NPC samples were prepared from polypyrrole (PPy) or by doping sawdust with melamine (SD-M). Finally, S-doped PC (SPC) samples were prepared from polythiophene (PTH). A summary of the materials studied including their surface chemical composition and textural characteristics is provided in Table 1. The precursors were characterized for comparison with the NPC and SPC samples (Table S1). We note that XPS only provides surface (and near surface) chemical composition that may differ from bulk chemical composition; however, surface composition is what matters in a surface adsorption process.

The high pressure volumetric  $\text{CO}_2$  adsorption uptake measurements were made in 1.5-1.8 bar increments up to 30 bar ( $3 \times 10^6$  Pa). A set of typical results is shown in Fig. 1. As may be seen, it is difficult to differentiate the performance of the NPC samples (PPy-T-2, where T = 500, 600, 700 and 800 °C) from the data collected below about 3-4 bar; however, at 10 bar the performance of each material is much easier to compare. The reproducibility batch-to-batch is sufficiently good to allow for comparisons between samples. For the purposes of the following discussion, the  $\text{CO}_2$  uptake at 30 bar is used.

### 3.1. Surface area and total pore volume

In creating an adsorbent with high gas uptake it is generally assumed that the higher the surface area and pore volume the better, and thus much research is aimed at increasing the surface area.<sup>41,54,55</sup> The surface area and pore volumes of the PC, NPC, and SPC samples was determined by  $\text{N}_2$  physisorption. A typical example of the  $\text{N}_2$  adsorption

**Table 1.** Summary of PC, NPC, and SPC samples studied with their elemental analysis, physical properties and CO<sub>2</sub> uptake.

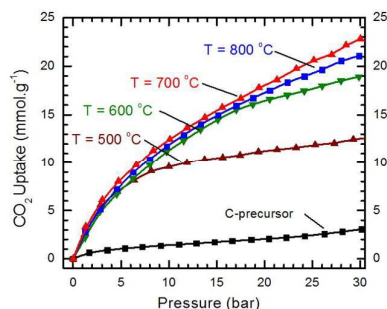
Sample <sup>a</sup>	C (wt%) <sup>b</sup>	O (wt%) <sup>b</sup>	N (wt%) <sup>b</sup>	S (wt%) <sup>b</sup>	Surface area S <sub>BET</sub> (m <sup>2</sup> g <sup>-1</sup> )	Total pore volume (cm <sup>3</sup> g <sup>-1</sup> ) <sup>c</sup>	CO <sub>2</sub> uptake at 30 bar and 24 °C (mmol.g <sup>-1</sup> )
Activated charcoal	94.10	5.90	0.00	0.00	845	0.43	8.45
BPL <sup>d</sup>	91.3	8.7	0.00	0.00	951	0.49	8.66
SD-600-4	82.24	15.80	0.00	0.00	2290	1.10	20.52
SD-800-4	89.96	8.03	0.00	0.00	2850	1.35	22.90
CN-600-2	88.13	11.87	0.00	0.00	1250	0.64	13.50
PPy-500-2	72.47	17.19	10.33	0.00	1255	0.53	12.60
PPy-600-2	74.78	19.72	5.49	0.00	2013	1.03	18.98
PPy-700-2	90.01	9.87	0.14	0.00	2956	1.45	22.98
PPy-800-2	91.39	8.60	0.00	0.00	3230	1.51	21.01
PPy-800-4	90.78	9.11	0.10	0.00	3450	2.57	22.10
PAn-600-3	84.50	6.75	8.75	0.00	1410	1.38	14.50
SD-M-800-4	85.39	8.15	6.46	0.00	2990	2.69	23.80
PTH-600-2	64.91	25.88	0.00	9.21	2256	1.02	18.81
PTH-700-2	82.47	13.01	0.00	4.51	1980	0.99	20.32
PTH-800-2	88.18	7.24	0.00	4.58	2890	1.43	22.87

<sup>a</sup> Precursor-temperature-KOH:precursor ratio. <sup>b</sup> Determined by XPS. <sup>c</sup> Determined at P/P<sub>0</sub> ~0.99. <sup>d</sup> Purchased from Calgon Carbon Corp.

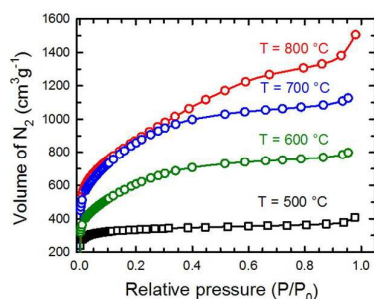
isotherms is shown in Fig. 2 for PPy-T-2 (where T = 500, 600, 700 and 800 °C).

Fig. 3a shows a plot of the uptake of CO<sub>2</sub> at 30 bar as a function of the apparent BET surface area (S<sub>BET</sub>) for all the PC adsorbent measured. As expected an increase in surface area

improvements in CO<sub>2</sub> uptake. In a similar manner, it is an intuitive assumption that increased total pore volume (V<sub>p</sub>) will facilitate increased CO<sub>2</sub> adsorption; however, as shown in Fig. 3b, it appears that for pore volumes tested over 1.35 cm<sup>3</sup>g<sup>-1</sup> there is not a resulting greater uptake.



**Fig. 1** CO<sub>2</sub> uptake as a function of CO<sub>2</sub> pressure on activated PPy-T-2 in comparison with the PPy precursor. Sorption measurements were performed at 24 °C.



**Fig. 2** N<sub>2</sub> adsorption isotherms for four different NPC samples PPy-T-2 prepared from polypyrrole and activated at the labelled temperature (T). Sorption measurements were performed at 24 °C.

correlates with an increase in CO<sub>2</sub> uptake; however, any value above 2800 m<sup>2</sup>g<sup>-1</sup> does not appear to improve adsorption. Thus, continued attempts to create even higher surface area materials will most likely not result in any further

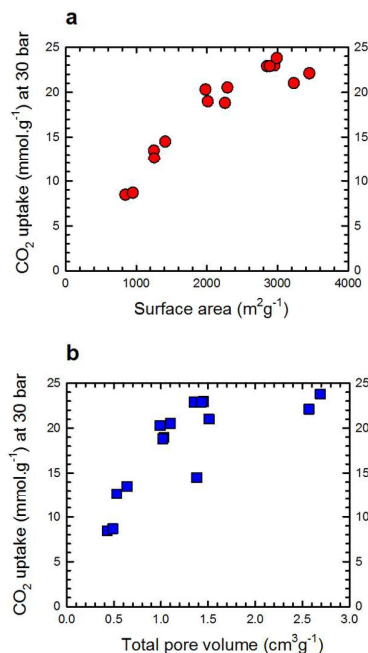


**Fig. 3** High pressure CO<sub>2</sub> uptake (@ 30 bar and 24 °C) as a function of the (a) surface area and (b) total pore volume, for a range of PC, NPC and SPC samples.

The trends noted above were for the highest pressures; however, the homologous series PPy-T-2 (T = 500, 600, 700, and 800 °C) along with the precursor (PPy) allows for a comparison across a range of pressures. Fig. 4 shows the relationship between CO<sub>2</sub> uptake and BET surface area (Fig. 4a) and total pore volume (Fig. 4b) for different pressures in the range of 5-30 bar. As expected, these plots clearly show a

significant effect of pressure on the CO<sub>2</sub> uptake, i.e., higher pressures result in higher uptake. However, what is interesting to note is that the point at which increased surface area (or total pore volume) does not increase CO<sub>2</sub> uptake decreases with decreased pressure. Thus, whereas at 30 bar CO<sub>2</sub> pressure increasing the surface area above 2800 m<sup>2</sup>g<sup>-1</sup> does not improve adsorption, at 5 bar this value decreases to 1300 m<sup>2</sup>g<sup>-1</sup> (Fig. 4a). This suggests a greater diminution of returns in attempting to create high surface area adsorbents if lower pressures are to be used in the system. The effect is similar for total pore volume, where at 5 bar it appears that any pore volume over 0.5 cm<sup>3</sup>g<sup>-1</sup> does not result in greater uptake.

There is a linear trend between surface area and pore volume for the majority of the samples studied (Fig. 5), but there are samples, which show a divergence from the trend. These all show a higher pore volume than expected and we note that these have some of the highest CO<sub>2</sub> uptake performance. The reasons for these divergences are discussed below.

### 3.2. Activation temperature and KOH concentration

The creation of high surface area PCs is generally accomplished by an oxidative activation step: steam, oxygen, or KOH. In the

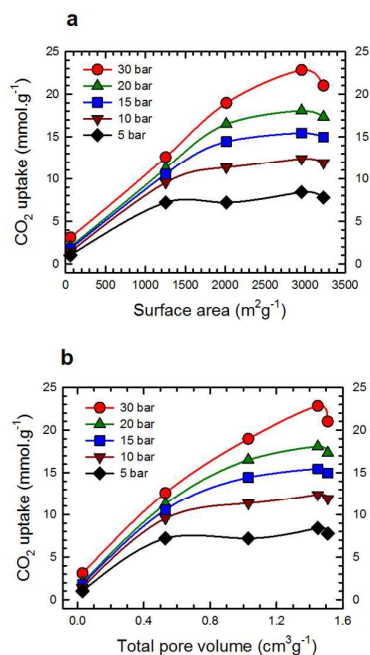


Fig. 4 Dependence of CO<sub>2</sub> uptake on (a) surface area and (b) total pore volume. PC samples were synthesized from polypyrrole and activated by KOH each at a different fixed temperature. Solid lines are only to guide the eye. Sorption measurements were performed at 24 °C.

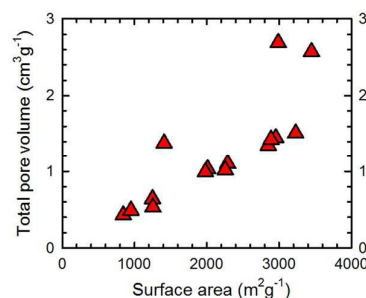


Fig. 5 Total pore volume as a function of surface area for a range of PC, NPC and SPC samples.

present study we have limited the activation to KOH. The advantage of this approach is that the resulting PC shows the highest CO<sub>2</sub> uptake; however, the disadvantage is that for the best results it is necessary to ensure complete mixing of the precursor and the KOH.

Fig. 6 shows the relationship between the activation temperature and the CO<sub>2</sub> uptake for the samples in Table 1. The general trend is increasing uptake with increased activation temperature with an possible maximum between 700 and 800 °C. Given the relationships between surface area and pore volume with CO<sub>2</sub> uptake, it is not surprising that their relationship with activation temperature is also similar (Fig. S1, see ESI).

The analysis of a series of samples prepared from PPy at different activation temperatures (i.e., PPy-T-2), but otherwise under identical conditions, allows for a convenient direct comparison of the effects of temperature. The CO<sub>2</sub> uptake plot for each sample as a function of CO<sub>2</sub> pressures is shown in Fig. 1, whereas Fig. 2 shows their corresponding N<sub>2</sub> adsorption isotherms at 77 K. It may be noticed that the shape of these isotherms is dependent on the activation temperature; the isotherm for PPy-800-2 is much steeper than that of PPy-500-2 between relative pressures of 0.4 and 1.0, indicating the variation in mesoporosity and adsorption capacity. For the homologous series of NPC materials the estimated surface area ( $S_{\text{BET}}$ ) and the total pore volume ( $V_{\text{p}}$ ) gradually increase with activation temperature (Fig. 7a and b) describing the incremental trend for mildly to strongly activated samples. Between 500 and 700 °C the surface area and total pore

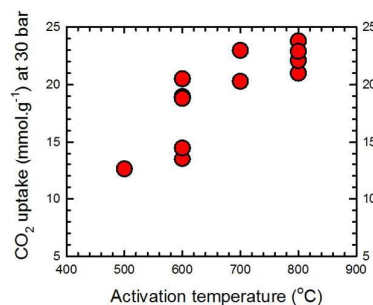
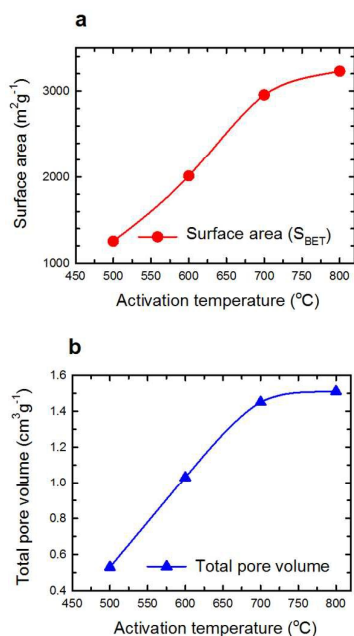


Fig. 6 Plot of CO<sub>2</sub> uptake at 30 bar and 24 °C as a function of activation temperature for PC, NPC and SPC samples.



**Fig. 7** Determination of pore structures by  $\text{N}_2$  physisorption isotherms of PPy-T-2 samples activated at different temperatures by  $\text{N}_2$  physisorption isotherms. (a) Estimated surface area and (b) total pore volume versus activation temperature.

volume increases systematically, whereas for temperatures above 700  $^{\circ}\text{C}$  no significant increment is noticed.

Besides the surface area and pore volume, another important characteristic that can be obtained from the  $\text{N}_2$  adsorption isotherms is the pore size distribution (PSD) of the porous solid. Fig. 8 depicts the PSDs for three different PPy-based PCs prepared under mild ( $T = 500$   $^{\circ}\text{C}$ ) to strong ( $T = 800$   $^{\circ}\text{C}$ ) activation conditions. The distribution plot for  $T = 500$   $^{\circ}\text{C}$  indicates that the activated PC mainly consists of micropores in the 1-2 nm range, whereas the plot for PPy-700-2 clearly shows signature of some larger pores in the 2-3.5 nm range. The most strongly activated PC, PPy-800-2, even shows significant number of mesopores in the 3-6 nm range, in agreement with the steeper adsorption registered for relative pressures  $>0.4$ .

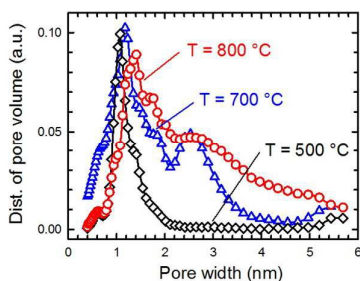


**Fig. 8** Pore size distributions of PPy-T-2 samples prepared at the three activation temperatures shown as determined by NLDFT method.

It is interesting to compare the variation in pore size and distribution (Fig. 8) with the  $\text{CO}_2$  uptake for the same samples

(Fig. 1 and Table 1). From 500  $^{\circ}\text{C}$  to 700  $^{\circ}\text{C}$  there is a dramatic increase in the high pressure uptake, which can be associated with the generation of pores in the range 2-3 nm; however as may be seen from Fig. 1 there is a slight (but significant) decrease upon further activation to 800  $^{\circ}\text{C}$  even though there is an increase in the presence of larger pores. This suggests that larger pores are not necessarily ideal for a high  $\text{CO}_2$  adsorption. The pore size distribution for the other top adsorbents studied shows a similar bi-modal pore structure centred on 1 nm and 1.5-2 nm (Fig. S2, see ESI).

The structural and textural morphology of the activated PPy-T-2 samples were characterized by scanning electron microscopy (SEM). Fig. 9a shows that the activated NPC contains multiple layers projected vertically upward and surfaces that are full of micron sized holes. In order to image the microporous structure of the activated sample, high resolution transmission electron microscopy (HRTEM) was utilized. Fig. 9b displays an image demonstrating randomly distributed micropores with dimensions in the range of 0.5-1 nm for a PPy-600-2 sample. These and the images of the other samples are in agreement with the BET measurements.

Given the hazardous nature of working with KOH, the amount used in the activation process is of importance with regard to any scalability issues. We have recently shown that KOH provides greater activation than borates.<sup>43</sup> In this regard, it is unfortunate that KOH appears to provide the best results,<sup>40</sup> and its action has been investigated in detail.<sup>9,12-14</sup>

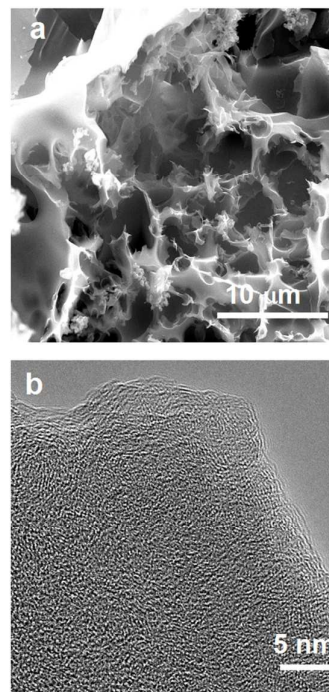


**Fig. 9** (a) Scanning electron microscope (SEM) and (b) High resolution transmission microscope (HRTEM) images of the PPy-600-2 sample.

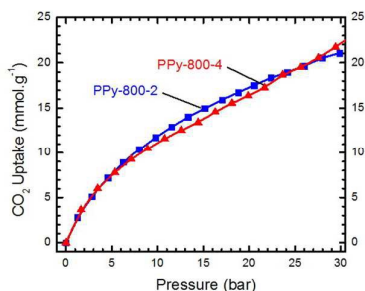


Fig. 10 High pressure volumetric  $\text{CO}_2$  adsorption uptake measurements on PPy-800-2 and PPy-800-4 showing the effect of the KOH:precursor ratio. Sorption measurements were performed at 24 °C.

However, based upon the present data set for PPy-800- $n$  ( $n = 2, 4$ ), it is clear that increasing the KOH:precursor ratio from 2 to 4 does not result in a change in the  $\text{CO}_2$  uptake profile (Fig. 10), despite a dramatic (70%) increase in the pore volume (Table 1). It should be noted that PPy-800-4 has one of the highest surface areas ( $3450 \text{ m}^2\text{g}^{-1}$ ) measured for any PC sorbent,<sup>11</sup> but is less efficient than PPy-800-4 between 10-20 bar. The effect of KOH concentration and mixing is the subject of further studies.

### 3.3. Heteroatom identity and content

As noted in the introduction it has been suggested that the high  $\text{CO}_2$  uptake observed for NPC and SPC at 30 bar is associated with the presence of the Lewis basic N and S centres.<sup>41</sup> We have therefore investigated the performance of NPC and SPC samples as a function of their heteroatom content.

The chemical composition of polypyrrole precursor and activated PPy derived NPC samples were determined by XPS (Table 1). The identity and wt% of the elements present on the sample surface were determined by XPS survey scans (e.g., Fig. 11a and b). These spectra revealed that the precursor polypyrrole and activated NPCs are primarily composed of C, O, and N. It should be noted that the O content of NPCs has been observed, but discounted as significant,<sup>41</sup> except as a potential source as both Lewis acid and base moieties.<sup>43</sup> We note that H content is not provided by XPS data, and so percentage values measured by other techniques will vary.

As a result of chemical activation and the activation temperature, the wt% of all elements changes (Table 1). The general trend is that the wt% of C increases, whereas that of O and N decreases gradually with increasing activation temperature. The compositional dependence on the activation temperature is demonstrated for the PPy-T-2 samples (Fig. 12). The first point to note is that the N content decreases consistently with activation temperature (Fig. 12b); however, there is a distinct step in the O composition between 600 and 700 °C (Fig. 12b), which is mirrored in the C wt% composition (Fig. 12a). However, it is important to note that while at the highest activation temperatures the N content becomes negligible, the O content remains significant.

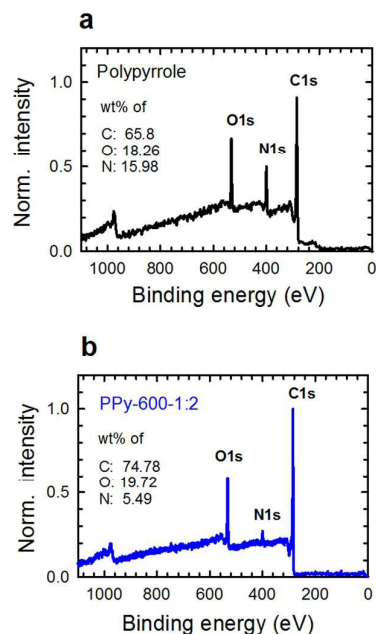


Fig. 11 Typical XPS survey scans for (a) the polypyrrole precursor and (b) PPy-600-2 NPC samples.

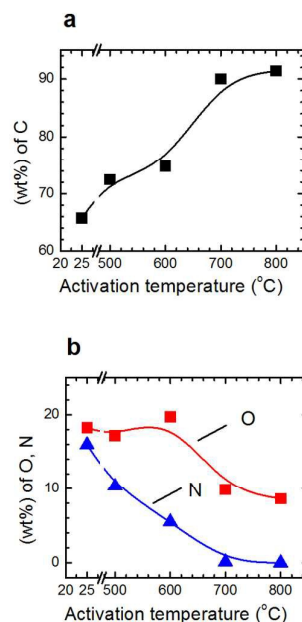


Fig. 12 The wt% determined by XPS of elemental (a) carbon and (b) oxygen and nitrogen versus activation temperature for the PPy precursor and PPy-T-2 samples.

An equally interesting variation was observed for SPC samples (Table 1). The C content stays essentially constant between the PTh precursor and the product activated at 600 °C, despite the S composition decreasing. The reason for this anomaly is the oxidation<sup>56</sup> of the PC material as measured by the increased O content. As with the N content in the NPC samples, the S composition in the SPC samples decreases to a



low value at the highest activation temperatures, but how do these changes correlate with CO<sub>2</sub> uptake?

The CO<sub>2</sub> uptake for NPC and SPC samples as a function of their N or S content is shown in Fig. 13. For both NPC and SPC samples the CO<sub>2</sub> uptake is at a maximum with the heteroatom content <5 wt%. Based upon these results it would appear that the presence of neither N nor S correlates in a positive manner with the CO<sub>2</sub> uptake, although in the present case a higher heteroatom content is associated to lower surface area and pore volume, hence the corresponding lower CO<sub>2</sub> uptake. Nonetheless, the limited effect of the presence of heteroatoms on CO<sub>2</sub> uptake is in line with previous results,<sup>37,46</sup> and our proposal that the presence of N or S is not responsible for any stabilization of poly-CO<sub>2</sub> that has been proposed to be responsible for high CO<sub>2</sub> adsorption at 30 bar.<sup>43</sup>

It is worth noting here that the source of the heteroatom also appears to affect the physical parameters and hence the CO<sub>2</sub> uptake. For example, the use of polyacrylonitrile (I, PAn) instead of polypyrrole (II, PPy) makes a significant difference suggesting the chemical speciation of the N content is important (Fig. 14a). In addition, the use of a poly-N containing heterocycle, melamine, as the N source results in an improvement in the performance (Fig. 14b). However, it is unclear whether this is a cause or effect. If the amount of CO<sub>2</sub> adsorbed is divided by the total pore volume one gets a similar value for both for PPy-800-4 and SD-M-800-4. Thus, the CO<sub>2</sub> uptake is determined by the total pore volume, but the pore volume is clearly a function of the precursor, rather than the process conditions.

As was noted with the pressure dependence of the CO<sub>2</sub> uptake on the surface area and total pore volume, the uptake

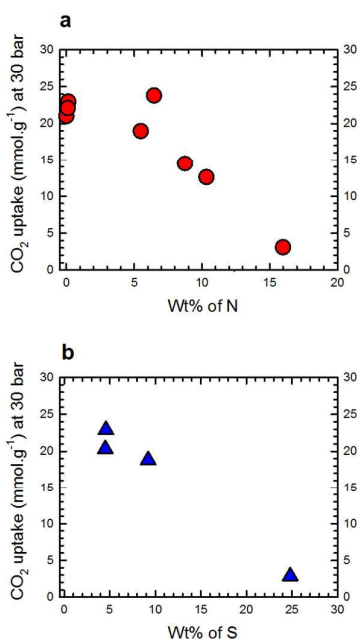


Fig. 13 High pressure (30 bar) CO<sub>2</sub> uptake as a function of (a) N wt% and (b) S wt% in NPC and SPC samples, respectively. Sorption measurements were performed at 24 °C.

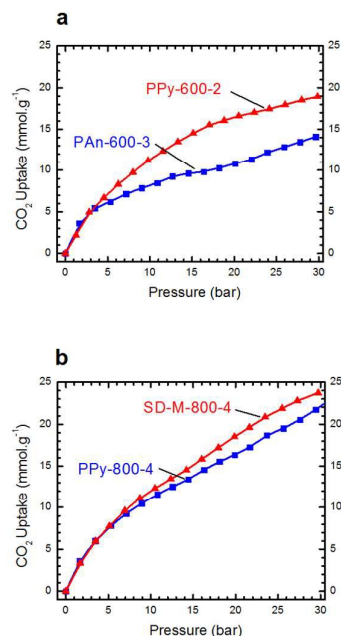


Fig. 14 High pressure CO<sub>2</sub> adsorption uptake for (a) PAn-600-3 compared with PPy-600-2 and (b) SD-M-800-4 compared with PPy-800-4. Sorption measurements were performed at 24 °C.

appears to be less affected by the N content at lower pressures. Thus, as shown in Fig. 15, the greatest CO<sub>2</sub> uptake at 30 bar for NPC requires N <2 wt%; however, if measured at 5 bar the uptake is almost independent of N content at values <10 wt%. This again suggests that the need to create specialty adsorbents diminishes with decreased operating pressure. Yet, this suggestion requires further study since in this case the N content and surface area (and total pore volume) are directly correlated, i.e., lower N content = larger surface area. In other words, the results presented here do not compare the effect of N-content at a fixed surface area and/or total pore volume. Nonetheless, the fact that at lower surface area a larger amount of N sites cannot keep the CO<sub>2</sub> uptake high could be the evidence of the limited capture effect of heteroatoms in PCs.

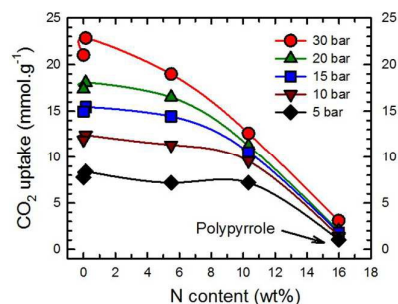


Fig. 15 Dependence of volumetric CO<sub>2</sub> uptake on N content for PPy-T-2 samples in comparison to the PPy precursor measured at different CO<sub>2</sub> pressures. Sorption measurements were performed at 24 °C.

Both NPC and SPC samples contain significant O, as do the PC samples produced from non-heteroatom containing precursors. Given that some of the PC samples perform in a comparable manner to those of NPC or SPC, N and S composition cannot be the sole key to high adsorption.<sup>43</sup> While the presence of >5 wt% of either N or S appears to significantly lower the uptake of CO<sub>2</sub>, although this could be related to the lower surface area of the heteroatom-rich samples, the O content is far more effective for the high CO<sub>2</sub> adsorption observed with 3-16 wt% O (Fig. 16a). In support to this observation, there are also some interesting findings on the CO<sub>2</sub> capture capacity of activated PCs obtained from the carbonization of asphalt with KOH.<sup>44</sup> The reduction with H<sub>2</sub> of asphalt-derived N-doped PCs causes a significant increase of capture capacity up to 26 mmol.g<sup>-1</sup>. The XPS elemental analysis of the sample before and after H<sub>2</sub> treatment shows that the sample with higher CO<sub>2</sub> capacity undergoes a significant increase of O content while the N content and type is only slightly changed.<sup>57</sup> This finding would support our hypothesis that O plays a major role in establishing the CO<sub>2</sub> capture capacity of PCs. However, what appears to be more important is the combined presence of a heteroatom, i.e., Σ(O,N,S), see Fig. 16b. This can be alternatively stated that the C content should be between 80-95 wt%.

Based upon the forgoing, it is possible to identify the parameters that define a PC material for maximum CO<sub>2</sub> uptake: have a surface area ≥2800 m<sup>2</sup>.g<sup>-1</sup>, a pore volume ≥1.35 cm<sup>3</sup>.g<sup>-1</sup>, and a C content between 80-95 wt%. To achieve these performance parameters it is necessary to activate above 700 °C and to ensure full mixing of the KOH with the precursor. The first two of these suggest that developing higher and higher

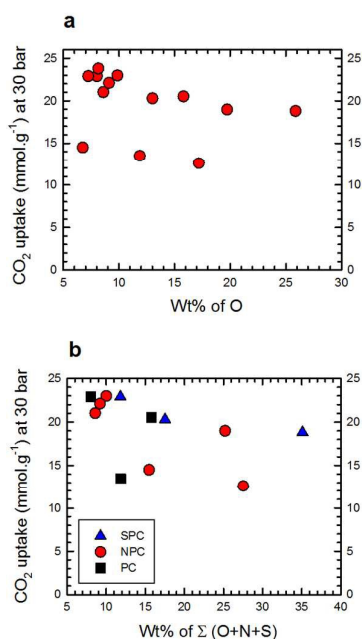


Fig. 16 The high pressure (30 bar) CO<sub>2</sub> uptake as a function of (a) O wt% and (b) Σ(O,N,S) wt% in PC, NPC and SPC samples. Sorption measurements were performed at 24 °C.

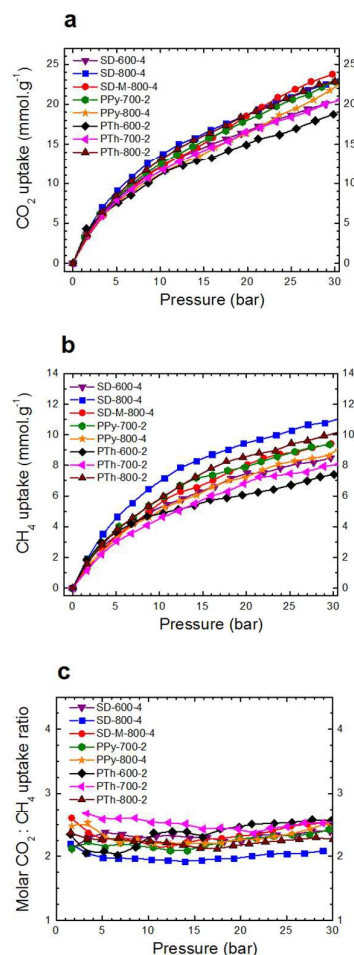


Fig. 17 Room temperature volumetric (a) CO<sub>2</sub> and (b) CH<sub>4</sub> adsorption isotherms for PC, NPC, and SPC samples. (c) The molar CO<sub>2</sub>:CH<sub>4</sub> uptake ratio as a function of gas pressure for PC, NPC, and SPC samples.

surface area materials is unproductive, and that understanding the third may lead to the design of new PC materials. Furthermore, these values offer additional variance when the uptake of CO<sub>2</sub> is required at lower pressures.

### 3.4. CO<sub>2</sub> versus CH<sub>4</sub> selectivity

The selective removal of CO<sub>2</sub> from natural gas, which essentially contains CH<sub>4</sub> and other gases such as CO<sub>2</sub>, H<sub>2</sub>S, and N<sub>2</sub>, is one of the important industrial processes, because these contaminant gases decrease power efficiency of the natural gas. The capture of CO<sub>2</sub> from natural gas primarily relies on purification strategies that allow the gas mixture to pass through a column packed with solid porous materials that captures CO<sub>2</sub> from the CH<sub>4</sub>-rich environment with minimal CH<sub>4</sub> uptake.

We have investigated the CO<sub>2</sub>/CH<sub>4</sub> selectivity by measuring CO<sub>2</sub> and CH<sub>4</sub> uptake isotherms up to a high pressure limit of 10, 20 and 30 bar at 24 °C. A summary of the data is shown in Table 2. Fig. 17a shows the CO<sub>2</sub> uptake plots along with the corresponding CH<sub>4</sub> uptake results in Fig. 17b. Additionally, the

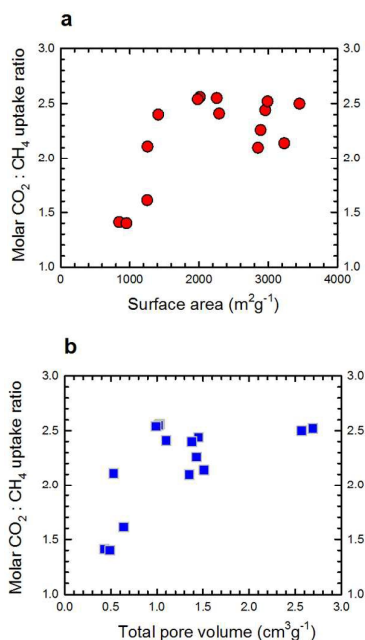


**Fig. 18** Plot of molar  $\text{CO}_2:\text{CH}_4$  uptake ratio (@ 30 bar) as a function of the (a) surface area and (b) total pore volume, for a range of PC, NPC and SPC samples. Sorption measurements were performed at 24 °C.

molar uptake selectivity ( $\text{CO}_2/\text{CH}_4$ ) is defined by the molar ratio of adsorbed  $\text{CO}_2$  and  $\text{CH}_4$  at a certain pressure, i.e., at 30 bar. The dependence of molar uptake selectivity for a sorbent as a function of corresponding gas pressure is depicted in Fig. 17c. For any particular sample, the selectivity varies with gas pressure. Of the samples investigated PPy-600-2 demonstrated highest selectivity of 2.56 at 30 bar.

Fig. 18a shows a plot of molar  $\text{CO}_2:\text{CH}_4$  uptake ratio as a function of the surface area ( $S_{\text{BET}}$ ) for all the PC adsorbents measured. For low surface area samples there is an increase in selectivity with increased surface area; however, as with uptake further increase in surface area above  $2000 \text{ m}^2\text{g}^{-1}$  does not appear to improve selectivity. In a similar manner, increased total pore volume ( $V_p$ ) does facilitate increased selectivity, but only to a pore volume of  $1.00 \text{ cm}^3\text{g}^{-1}$ , above this there is no improvement in performance (Fig. 18b).

The series PPy-T-2 ( $T = 500\text{--}800 \text{ }^\circ\text{C}$ ) allows for the direct comparison of homologous materials. In this case it appears that the values of  $2000 \text{ m}^2\text{g}^{-1}$  and  $1.00 \text{ cm}^3\text{g}^{-1}$  for the surface area and total pore volume (Fig. 19) represent maxima rather thresholds. It is possible that for any homologous series similar maxima are observed; however, the thresholds observed in Fig. 18 are useful indicators. From Table 2 it can be seen that an activation temperature of  $600 \text{ }^\circ\text{C}$  is a minimum for good selectivity; however, from Fig. 19c it may be seen that for the series PPy-T-2 ( $T = 500\text{--}800 \text{ }^\circ\text{C}$ ) this value is actually an optimum. Again this may vary with a particular class of material, but a lower activation temperature is required to create a material with good selectivity as compared to

optimum  $\text{CO}_2$  uptake (Fig. 19d), suggesting that the best attainable sorbent material will have to combine a wise trade-off of selectivity and  $\text{CO}_2$  capture capacity. As may be seen from a comparison of PPy-800-2 and PPy-800-4 (Table 2), increased KOH concentration during the activation step results in greater selectivity. This is undoubtedly due to an increased O content, see below.

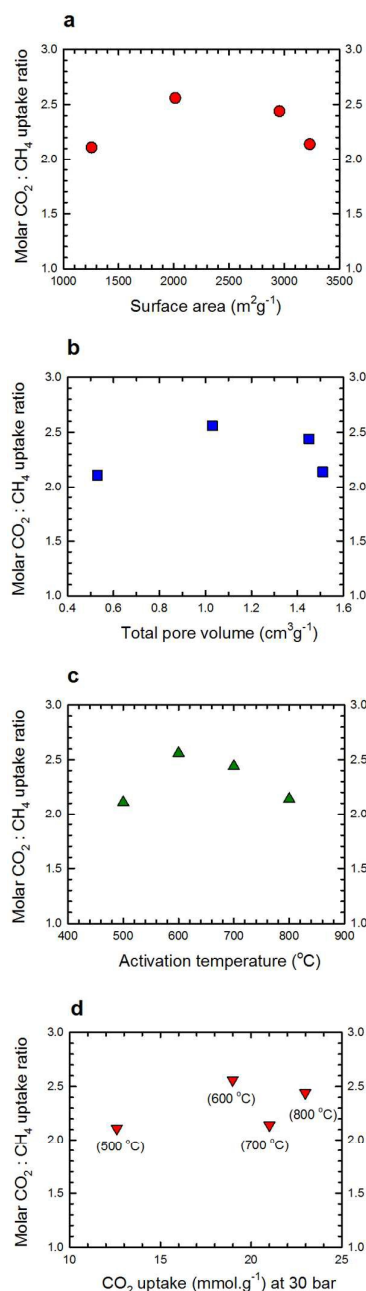


**Fig. 19** Plot of molar  $\text{CO}_2:\text{CH}_4$  uptake ratio (@ 30 bar) as a function of the (a) surface area, (b) total pore volume, (c) activation temperature, and (d)  $\text{CO}_2$  uptake for PPy-T-2 ( $T = 500, 600, 700$  and  $800 \text{ }^\circ\text{C}$ ) NPC samples. Sorption measurements were performed at 24 °C.

**Table 2.** Summary of PC, NPC, and SPC samples studied with their molar gas uptakes and selectivity for CO<sub>2</sub> over CH<sub>4</sub> at different uptake pressures.

Sample <sup>a</sup>	CO <sub>2</sub> uptake (mmol.g <sup>-1</sup> ) at			CH <sub>4</sub> uptake (mmol.g <sup>-1</sup> ) at			Molar (CO <sub>2</sub> :CH <sub>4</sub> ) uptake ratio		
	10 bar	20 bar	30 bar	10 bar	20 bar	30 bar	10 bar	20 bar	30 bar
Activated charcoal	6.27	7.51	8.45	4.28	5.44	6.03	1.46	1.38	1.41
BPL	6.30	7.87	8.66	3.24	4.96	6.18	1.94	1.59	1.40
SD-600-4	12.06	16.77	20.52	5.23	7.54	8.52	2.31	2.22	2.41
SD-800-4	13.61	18.78	22.90	6.65	9.45	10.92	2.05	1.99	2.10
CN-600-2	10.91	12.65	13.50	5.94	7.24	7.96	1.83	1.74	1.70
PPy-500-2	9.51	11.27	12.60	4.11	5.06	5.98	2.31	2.23	2.11
PPy-600-2	11.37	16.45	18.98	5.39	6.33	7.41	2.11	2.60	2.56
PPy-700-2	12.50	18.12	22.98	5.75	7.92	9.41	2.17	2.29	2.44
PPy-800-2	11.94	17.21	21.01	5.78	8.23	9.82	2.07	2.09	2.14
PPy-800-4	11.18	16.51	22.11	5.10	7.33	8.83	2.19	2.25	2.50
PAn-600-3	8.19	10.84	14.50	4.04	5.26	6.03	2.03	2.06	2.40
SD-M-800-4	12.09	18.70	23.76	5.58	8.12	9.41	2.17	2.30	2.52
PTH-600-2	11.17	15.42	18.81	4.77	6.12	7.37	2.34	2.52	2.55
PTH-700-2	11.51	16.67	20.32	4.62	6.87	8.01	2.49	2.43	2.54
PTH-800-2	13.10	18.80	22.87	5.81	8.55	10.14	2.25	2.20	2.26

<sup>a</sup> Precursor-temperature-KOH:precursor ratio.

The molar CO<sub>2</sub>:CH<sub>4</sub> uptake ratio for NPC samples as a function of their N content is shown in Fig. 20. The selectivity for measurements at 30 bar decreases with N content above 5 wt%. In the case of SPC, there appears to be no effect on selectivity with S content (Tables 1 and 2). These results seem to suggest that the presence of neither N nor S correlates in a direct manner with the CO<sub>2</sub>/CH<sub>4</sub> selectivity. This is in line with our previous proposal.<sup>43</sup> Although, we need to recall that in this work a higher heteroatom content implies a lower surface area (and total pore volume) of the sorbent materials, hence a definite lack of impact of N or S doping on the selectivity

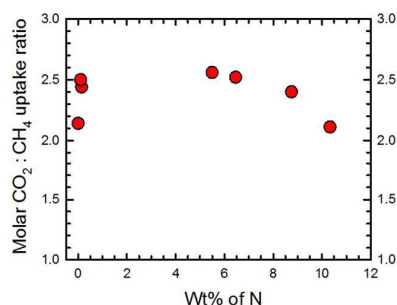


**Fig. 20** The high pressure (30 bar) molar CO<sub>2</sub>:CH<sub>4</sub> uptake ratio as a function of N wt% in NPC samples. Sorption measurements were performed at 24 °C.

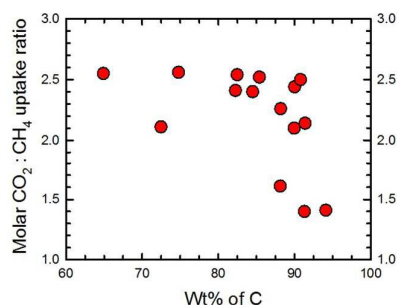


**Fig. 21** The high pressure (30 bar) molar CO<sub>2</sub>:CH<sub>4</sub> uptake ratio as a function of C wt% in PC, NPC, and SPC samples. Sorption measurements were performed at 24 °C.

performance of in PCs cannot be considered a priori. Interestingly, as may be seen from the data in Table 2, at lower pressures (10 bar) there is almost no dependence between selectivity and heteroatom content.

As was observed with the uptake efficiency for CO<sub>2</sub>, the selectivity appears to be more a function of the total heteroatom composition, i.e., Σ(O,N,S) wt%, as presented in Fig. 21 in terms of C wt% (= 100 - Σ(O,N,S) wt%). However, based upon the analysis of all the PC, NPC, and SPC materials studied, the O wt% seems to be the major contributor. The CO<sub>2</sub>/CH<sub>4</sub> selectivity is at a potential maximum as long as C content is below 90 wt%, i.e., for Σ(O,N,S) > 10 wt%. At lower pressure (10 bar) the carbon content is possibly even higher, C < 94 wt%.

## Conclusions

A study of a wide range of PC, NPC, and SPC materials under high pressure CO<sub>2</sub> and CH<sub>4</sub> adsorption offers some useful insight into the parameters that may collectively control both the CO<sub>2</sub> uptake efficiency and the CO<sub>2</sub>/CH<sub>4</sub> selectivity. A summary of the proposed key requirements for a PC material with either good CO<sub>2</sub> uptake or good CO<sub>2</sub>/CH<sub>4</sub> selectivity is given in Table 3 based on the results presented herein.

As far as CO<sub>2</sub> uptake is concerned any porous carbon material with a surface area >2800 m<sup>2</sup>g<sup>-1</sup> at 30 bar is unlikely to be bettered (when prepared from the KOH activation of a non-nanostructured precursors). A similar threshold appears to be true for the total pore volume of the material (1.35 cm<sup>3</sup>g<sup>-1</sup>). This suggests that seeking synthetic routes to ever higher surface area and/or high pore volume PC-based adsorbents is counterproductive.<sup>39</sup> However, it should be understood that if uptake at lower pressures is desired these threshold values decrease even further. This result is highly important in considering the choice of adsorbent to be used in a large scale unit.<sup>58</sup> The adsorbent intended for use in a low pressure system needs a lower surface area and pore volume to perform than a potentially more expensive to manufacture material. It also impacts the formation of pelletized materials

for fluid bed applications, since the formation of the pellet through inclusion of a binder inevitably lowers the surface area and pore volume.<sup>39</sup> Our results suggest that for lower pressure applications this is not important since the uptake is less dependent on extremely high surface areas and/or pore volumes.

**Table 3.** Summary of proposed parameters required for optimum CO<sub>2</sub> uptake and CO<sub>2</sub>/CH<sub>4</sub> selectivity for PC, NPC, and SPC.

Parameter	Uptake @ 30 bar	Selectivity @ 30 bar
Surface area (m <sup>2</sup> g <sup>-1</sup> )	>2800	>2000
Total pore volume (cm <sup>3</sup> g <sup>-1</sup> )	>1.35	>1.0
Temperature of activation (°C)	700-800	600
Carbon content (%)	80-95	<90

Given the prior interest in N- and S-doped PC materials, the results show that CO<sub>2</sub> uptake is inversely related to S and N content in SPC and NPC, respectively. However, it is essential to underline that this conclusion is 'preparation process'-specific. In other words, due to the preparation process used in this study (KOH activation), there is an intrinsic dependence between heteroatom content and surface area (total pore volume) in all sorbents, i.e., higher surface areas imply lower N or S contents. Consequently, the use of KOH activated PCs in industrial scale units, must take into account that a higher heteroatom content cannot offset the corresponding drop of CO<sub>2</sub> capture performance due to a decrease of surface area of the materials. In practical terms, it is the  $\Sigma(\text{O,N,S})$  wt% or C wt% (= 100 -  $\Sigma(\text{O,N,S})$  wt%) that is the defining factor for CO<sub>2</sub> uptake. This is true irrespective of the source of the heteroatom; however, O appears to be the main factor, since a C content of between 80 and 95 wt% offers the potential for high CO<sub>2</sub> uptake, but at these levels if the make-up is N or S the uptake is likely reduced. It should also be observed based upon the source of the heteroatom that if heteroatoms are to be incorporated and "active" they are preferentially included using heterocycle precursors, such as melamine in the case of N, rather than other heteroatom-rich structures. A recent study of cotton derived porous carbon in comparison with its oxidized analogue shows that the O content appears to enhance removal of metal ions from solution.<sup>59</sup>

It may be assumed that the parameters that makes a good CO<sub>2</sub> adsorbent may be the same as those that make a selective material; however, our results indicate that the two are only broadly related. The levels of surface area and pore volume can be even lower for good CO<sub>2</sub>/CH<sub>4</sub> selectivity, as compared to CO<sub>2</sub> uptake, see Table 3.

In summary, we can conclude that a synthetic goal for PC-based material, for both high CO<sub>2</sub> adsorption and high CO<sub>2</sub>/CH<sub>4</sub> selectivity, would comprise a C content of less than 90%. Given that neither N nor S seem to have a significant effect rather than the O that is present,<sup>43</sup> it is clear that a design C<sub>x</sub>O<sub>1-x</sub> where x < 0.9 would possibly make an ideal CO<sub>2</sub> adsorbent material with the best CO<sub>2</sub>/CH<sub>4</sub> selectivity. Furthermore, the goal should be a precursor where oxygen is incorporated into a cyclic moiety. This is therefore the goal of our future research.

## Acknowledgements

Financial support was provided by Apache Corporation, Inc, the Welsh Government Sêr Cymru Programme and the Robert A. Welch Foundation (C-0002). M. S. acknowledges funding by the Spanish Ministerio de Economía y Competitividad, MINECO (MAT2012-31651), and Fondo Europeo de Desarrollo Regional (FEDER), and thanks the Spanish Ministerio de Ciencia e Innovación for her Ramón y Cajal contract. The authors declare no conflict of interest.

## Notes and references

- 1 IPCC Fourth Assessment Report: Climate Change 2007 (AR4), Intergovernmental Panel on Climate Change, Geneva, Switzerland, 2007.
- 2 CO<sub>2</sub> Emissions from Fuel Combustion-Highlights, International Energy Agency, Paris, France, 2012.
- 3 B. Metz, H. de Coninck, M. Loos, L. Meyer, Eds., *Carbon Dioxide Capture and Storage*. Intergovernmental Panel on Climate Change, Cambridge University Press, 2005.
- 4 M. Z. Jacobson, *Energy Environ. Sci.*, 2009, **2**, 148-173.
- 5 N. von der Assen, P. Voll, M. Peters, and A. Bardow, *Chem. Soc. Rev.*, 2014, **43**, 7982-7994.
- 6 S. Rackley, *Carbon capture and storage*. Butterworth-Heinemann, Oxford, 2009.
- 7 A. Yamasaki, *J. Chem. Eng. Jpn.*, 2003, **36**, 361-375.
- 8 I. B. Strachan, K. A. Nugent, S. Crombie, and M.-C. Bonneville, *Environ. Res. Lett.*, 2015, **10**, 065006.
- 9 J. Lehmann, M. C. Rillig, J. Thies, C. A. Masiello, W. C. Hockaday, and D. Crowley, *Soil Biol. Biochem.*, 2011, **43**, 1812-1836.
- 10 D. Aaron and C. Tsouris, *Sep. Sci. Technol.*, 2005, **40**, 321-348.
- 11 Z. Yong, V. Mata, and A. E. Rodrigues, *Sep. Purific. Technol.*, 2002, **26**, 195-205.
- 12 T. E. Rufford, S. Smart, G. C. Y. Watson, B. F. Graham, J. Boxall, J. C. Diniz da Costa, and E. F. May, *J. Petr. Sci. Eng.*, 2012, **94-95**, 123-154.
- 13 Z. Y. Yeo, T. L. Chew, P. W. Zhu, A. R. Mohamed, and S. P. Chai, *J. Nat. Gas Chem.*, 2012, **21**, 282-298.
- 14 A. Bahadori, S. Mokhtab, and B. F. Towler, *J. Nat. Gas Chem.*, 2007, **16**, 349-353.
- 15 A. B. Rao and E. S. Rubin, *Environ. Sci. Technol.*, 2002, **36**, 4467-4475.
- 16 M. R. M. Abu-Zahra, L. H. J. Schneiders, J. P. M. Niederer, P. H. M. Feron, and G. F. Versteeg, *Int. J. Greenh. Gas Contr.*, 2007, **1**, 37-46.
- 17 K. Veltman, B. Singh, and E. G. Hertwich, *Environ. Sci. Technol.*, 2010, **44**, 1496-1502.
- 18 C. J. Nielsen, H. Herrmann, and C. Weller, *Chem. Soc. Rev.*, 2012, **41**, 6684-6704.
- 19 G. T. Rochelle, *Science*, 2009, **325**, 1652-1654.
- 20 D. M. D'Alessandro, B. Smit, and J. R. Long, *Angew. Chem. Int. Ed.*, 2010, **49**, 6058-6082.
- 21 S. Choi, J. H. Drese, and C. W. Jones, *ChemSusChem.*, 2009, **2**, 796-854.
- 22 E. P. Dillon, E. Andreoli, L. Cullum, and A. R. Barron, *J. Exp. Nanosci.*, 2015, **10**, 746-768.
- 23 E. Andreoli and A. R. Barron, *Energy Fuels*, 2015, **29**, 4479-4487.
- 24 E. Andreoli and A. R. Barron, *ChemSusChem*, 2015, **8**, 2635-2644.
- 25 M. Ramdin, T. W. de Loos, and T. J. H. Vlugt, *Ind. Eng. Chem. Res.*, 2012, **51**, 8149-8177.
- 26 X. P. Zhang, X. C. Zhang, H. F. Dong, Z. J. Zhao, S. J. Zhang, and Y. Huang, *Energy Environ. Sci.*, 2012, **5**, 6668-6681.

- 27 S. P. Wang, S. L. Yan, X. B. Ma, and J. L. Gong, *Energy Environ. Sci.* **2011**, *4*, 3805-3819.
- 28 A. Samanta, A. Zhao, G. K. H. Shimizu, P. Sarkar, and R. Gupta, *Ind. Eng. Chem. Res.*, **2012**, *51*, 1438-1463.
- 29 M. Sevilla and A. B. Fuertes, *Energy Environ. Sci.*, **2011**, *4*, 1765-1771.
- 30 A. R. Millward, and O. M. Yaghi, *J. Am. Chem. Soc.*, **2005**, *127*, 17998-17999.
- 31 J. R. Li, Y. Ma, M. C. McCarthy, J. Sculley, J. Zu, H. K. Jeong, P. B. Balbuena, and H. C. Zhou, *Coord. Chem. Rev.*, **2011**, *255*, 1791-1823.
- 32 R. E. Morris and P. S. Wheatley, *Angew. Chem. Int. Edit.*, **2008**, *47*, 4966-4981.
- 33 S. Araki, H. Doi, Y. Sano, S. Tanaka, and Y. Miyake, *J. Colloid Interface Sci.*, **2009**, *339*, 382-389.
- 34 J. Liu, P. K. Thallapally, B. P. McGrail, D. R. Brown, and J. Liu, *Chem. Soc. Rev.*, **2012**, *41*, 2308-2322.
- 35 M. Sevilla, P. Valle-Vigón, and A. B. Fuertes, *Adv. Funct. Mater.*, **2011**, *21*, 2781-2787.
- 36 M. Sevilla and A. B. Fuertes, *Micropor. Mesopor. Mat.*, **2012**, *158*, 318-323.
- 37 M. Sevilla, J. B. Parra, and A. B. Fuertes, *ACS Appl. Mater. Interfaces*, **2013**, *5*, 6360-6368.
- 38 G. P. Hao, W. C. Li, D. Qian, and A. H. Lu, *Adv. Mater.*, **2010**, *22*, 853-857.
- 39 A. S. Ello, J. A. Yapó, and A. Trokourey, *Afr. J. Pure Appl. Chem.*, **2013**, *7*, 61-66.
- 40 V. Chandra, S. U Yu, S. H. Kim, Y. S. Yoon, D. Y. Kim, A. H. Kwon, M. Meyyappan, and K. S. Kim, *Chem. Commun.* **2012**, *48*, 753-737.
- 41 C. C. Hwang, J. J. Tour, C. Kittrell, L. Espinal, L. B. Alemany, and J. M. Tour, *Nat. Commun.*, **2014**, *5*, 1-6.
- 42 M. Sevilla, A. B. Fuertes, and R. Mokaya, *Int. J. Hydrogen Energ.*, **2011**, *36*, 15658-15663.
- 43 S. Ghosh and A. R. Barron, *C*, **2016**, *2*, 5.
- 44 E. Carmona, F. González, M. L. Poveda, and J. M. Marin, *J. Am. Chem. Soc.*, **1983**, *105*, 3365-3366.
- 45 J. Langer, W. Imhof, M. J. Fabra, P. García-Orduna, H. Görls, F. J. Lahoz, L. A. Oro, and M. Westerhausen, *Organometallics*, **2010**, *29*, 1642-1651.
- 46 B. Adeniran and R. Mokaya, *Chem. Mater.*, **2016**, *28*, 994-1001.
- 47 E. Andreoli, E. P. Dillon, L. Cullum, L. B. Alemany, and A. R. Barron, *Sci. Rep.*, **2014**, *4*, 7304.
- 48 F. Dreisbach, R. Staudt, and J. U. Keller, *Adsorption*, **1999**, *5*, 215-227.
- 49 B. M. Krooss, F. van Bergen, Y. Gensterblum, H. J. M. Pagnier, and P. David, *Int. J. Coal Geol.*, **2002**, *51*, 69-92.
- 50 J.-S. Bae and S. K. Bhatia, *Energy Fuels*, **2006**, *20*, 2599-2607.
- 51 S. Himeno, T. Komatsu, and S. Fujita, *J. Chem. Eng. Data*, **2005**, *50*, 369-376.
- 52 W. Shen, S. Zhang, Y. He, J. Li, and W. Fan, *J. Mater. Chem.*, **2011**, *21*, 14036-14040.
- 53 J. Landers, G. Yu, and A. V. Neimark, *Colloids Surf.*, **2013**, *A437*, 3-32.
- 54 H.-L. Jiang, B. Liu, Y.-Q. Lan, K. Kurantani, T. Akita, H. H. Shioyama, F. Zong, and Q. Xu, *J. Am. Chem. Soc.*, **2011**, *133*, 11854-11857.
- 55 Y. Xia, R. Mokaya, G. S. Walker, and Y. Zhu, *Adv. Energy Mater.*, **2011**, *1*, 678-683.
- 56 J. Wang and S. Kaskel, *J. Mat. Chem.*, **2012**, *22*, 23710-23725.
- 57 A. S. Jalilov, G. Ruan, C.-C. Hwang, D. E. Schipper, J. J. Tour, Y. Li, H. Fei, E. L. G. Samuel, and J. M. Tour, *ACS Appl. Mater. Interfaces*, **2015**, *7*, 1376-1382.
- 58 M. T. Ho, G. W. Allinson, and D. E. Wiley, *Ind. Eng. Chem. Res.*, **2008**, *47*, 4883-4890.
- 59 H. Chen, X. Wang, J. Li and X. Wang, *J. Mater. Chem. A*, **2015**, *3*, 6073-6081.

## Graphical Abstract

